

# Photoproduction of $K^*\Sigma$ in an effective Lagrangian approach

Fei Huang<sup>1,\*</sup>, Ai-Chao Wang<sup>1,2</sup>, and Neng-Chang Wei<sup>1,3</sup>

<sup>1</sup>School of Nuclear Science and Technology, University of Chinese Academy of Sciences, Beijing 101408, China

<sup>2</sup>College of Science, China University of Petroleum (East China), Qingdao 266580, China

<sup>3</sup>School of Physics, Henan Normal University, Henan 453007, China

**Abstract.** All the available data on differential cross sections, total cross sections, spin density matrix elements, and parity spin asymmetry for the  $\gamma p \rightarrow K^{*+}\Sigma^0$  and  $\gamma p \rightarrow K^{*0}\Sigma^+$  reactions are analyzed within an effective Lagrangian approach. The reaction amplitudes are constructed by considering the *s*-channel exchanges of  $N$ ,  $\Delta$ , and their excited states, the *t*-channel exchanges of  $K$ ,  $K^*$ , and  $\kappa$ , the *u*-channel exchanges of  $\Lambda$ ,  $\Sigma$ , and  $\Sigma^*$ , and the interaction current. Two fits with different reaction mechanisms are obtained that describe the data equally well. The *s*-channel  $\Delta(1905)5/2^+$  resonance exchange is found to provide dominant contributions in both fits. The *t*-channel  $\kappa$  exchange only contributes significantly to  $\gamma p \rightarrow K^{*0}\Sigma^+$  in model II, which challenges the claim made in literature that the available parity spin asymmetry data supports the dominant contribution of  $\kappa$  exchange in  $\gamma p \rightarrow K^{*0}\Sigma^+$ .

## 1 Introduction

Extraction  $N^*$ 's from data and understanding their nature are essential to our understanding of the non-perturbative behavior of QCD. Our current knowledge of most of the  $N^*$ 's is coming from  $\pi N \rightarrow \pi N$  scattering and  $\gamma N \rightarrow \pi N$ ,  $KY$  ( $Y = \Lambda, \Sigma$ ) reactions. It is known that some  $N^*$ 's may couple weakly to  $\pi N$  and  $KY$  but strongly to other channels. Thus, much efforts have been made in studying  $N^*$ 's from the production reactions of mesons other than  $\pi$  and  $K$  in the past few years. In the present work, we concentrate on the photoproduction of  $K^*\Sigma$ , whose threshold is much higher than that of  $\pi N$  and thus is more suitable to study  $N^*$ 's with higher masses in the less explored energy region.

Experimentally, for  $\gamma p \rightarrow K^{*+}\Sigma^0$ , we have differential cross-section and total cross-section data in the energy region from threshold up to center-of-mass energy  $W = 2814$  MeV published in 2013 by the CLAS Collaboration [1]. For  $\gamma p \rightarrow K^{*0}\Sigma^+$ , we have differential cross-section data in the energy region from threshold up to  $W = 2519$  MeV published in 2007 by the CLAS Collaboration [2] and  $W = 2321$  MeV published in 2008 by the CBELSA/TAPS Collaboration [3], and the data on spin density matrix elements and parity spin asymmetry at  $W = 2087 \sim 2538$  MeV published in 2012 by the LEPS Collaboration [4].

Theoretically, many works have already been devoted to the study of  $K^*\Sigma$  photoproduction reactions [5–9]. In Ref. [5], predictions of differential cross sections, total cross sections, and beam asymmetries for  $\gamma p \rightarrow K^{*+}\Sigma^0$  and  $\gamma p \rightarrow K^{*0}\Sigma^+$  were made in a quark model

\* e-mail: huangfei@ucas.ac.cn

with an effective Lagrangian. In Ref. [6], differential and total cross sections for  $\gamma p \rightarrow K^{*0}\Sigma^+$  were calculated in an effective Lagrangian approach and compared with the preliminary (unpublished) data, and the parity spin asymmetry for  $\gamma p \rightarrow K^{*0}\Sigma^+$  were predicted, based on which it was claimed that the  $\kappa$  exchange is substantial for this reaction. In Ref. [7], the differential and total cross sections for  $\gamma p \rightarrow K^{*+}\Sigma^0$  and  $\gamma p \rightarrow K^{*0}\Sigma^+$  were computed within an effective Lagrangian approach and compared with the data. It was concluded that the resonance contributions are negligible while the contributions from  $K$  and  $\Delta$  exchanges are dominant for  $K^*\Sigma$  photoproduction reactions. In Ref. [8], a combined analysis of the  $\gamma p \rightarrow K^{*+}\Sigma^0$  and  $\gamma p \rightarrow K^{*0}\Sigma^+$  reactions was performed within an effective Lagrangian approach, and a much better description of the data on differential and total cross sections, compared with previous theoretical results, was achieved. It was found that the  $\Delta(1905)5/2^+$  resonance is rather important for  $K^*\Sigma$  photoproduction. In Ref. [9], the  $N(2080)3/2^-$  and  $N(2270)3/2^-$  molecules were introduced to replace the  $\Delta(1905)5/2^+$  resonance in Ref. [8], and it was found that the data can still be well reproduced, indicating that the molecular structures of  $N(2080)3/2^-$  and  $N(2270)3/2^-$  are compatible with the  $K^*\Sigma$  photoproduction data.

It is noticed that the reaction mechanisms extracted from various theoretical works [5–9] are not convergent. Moreover, the LEPS data [4] on spin density matrix elements and parity spin asymmetry for  $\gamma p \rightarrow K^{*0}\Sigma^+$  have never been theoretically analyzed in literature. In the present work, we perform a combined analysis of all the available data for  $\gamma p \rightarrow K^{*+}\Sigma^0$  and  $\gamma p \rightarrow K^{*0}\Sigma^+$  within an effective Lagrangian approach, with the purpose being to understand the reaction mechanism, especially, the role of resonance and  $\kappa$  exchanges in  $K^*\Sigma$  photoproduction.

## 2 The model

We consider the  $s$ -channel exchanges of  $N$ ,  $\Delta$ , and their excited states, the  $t$ -channel exchanges of  $K$ ,  $K^*$ , and  $\kappa$ , the  $u$ -channel exchanges of  $\Lambda$ ,  $\Sigma$ , and  $\Sigma^*$ , and the interaction current to construct the reaction amplitudes for  $K^*\Sigma$  photoproduction. After numerical trials it was found that by including in  $s$  channel the  $\Delta(1905)5/2^+$  resonance the data can be well reproduced. The full photoproduction amplitudes can be written as

$$M^{\nu\mu} = M_s^{\nu\mu} + M_t^{\nu\mu} + M_u^{\nu\mu} + M_{\text{int}}^{\nu\mu}, \quad (1)$$

where  $\nu$  and  $\mu$  are Lorentz indices of vector meson  $K^*$  and photon  $\gamma$ , respectively. All these four diagrams in Eq. (1) are schematically depicted in Fig. 1. The  $s$ -,  $t$ -, and  $u$ -channel amplitudes, i.e.  $M_s^{\nu\mu}$ ,  $M_t^{\nu\mu}$ , and  $M_u^{\nu\mu}$ , can be constructed straightforwardly by computing the corresponding Feynman diagrams. The interaction current,  $M_{\text{int}}^{\nu\mu}$ , is constructed in such a way that the full photoproduction amplitude satisfies the generalized Ward-Takahashi identity and thus is really gauge invariant. The model parameters include the cutoff parameters for the  $N$ ,  $\Delta$ ,  $\Sigma^*$ ,  $\Lambda$ ,  $\Sigma$ ,  $K$ ,  $\kappa$ , and  $K^*$  exchanges, the coupling constants for the  $\Delta\Sigma K^*$  and  $\Sigma^*\Sigma$

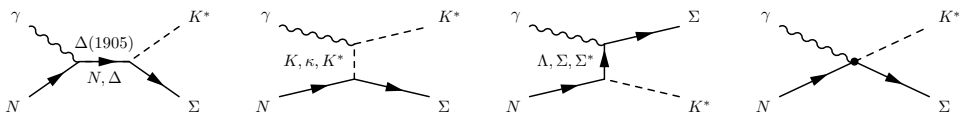


**Figure 1.** Generic structure of the  $K^*$  photoproduction amplitude for  $\gamma N \rightarrow K^*\Sigma$ . The four subfigures correspond to the diagrams for  $s$ -,  $t$ -, and  $u$ -channel interactions and the interaction current, respectively. Time proceeds from left to right.

vertices, and the mass, width, helicity amplitudes, hadronic couplings, and cutoff parameter for the  $N(1905)5/2^+$  resonance contributions. Their values are determined through fitting the available data for  $K^*\Sigma$  photoproduction reactions by use of MINUIT. More details of the model are referred to Refs. [8, 10].

### 3 Results and discussion

We perform a combined analysis of all the available data on differential cross sections, spin density matrix elements, and parity spin asymmetry for  $\gamma p \rightarrow K^{*+}\Sigma^0$  and  $\gamma p \rightarrow K^{*0}\Sigma^+$  in an effective Lagrangian approach. The  $\Delta(1905)5/2^+$  resonance is found to be needed to describe the data. Two solutions with similar fitting qualities are achieved, named as model I and model II in the following parts.

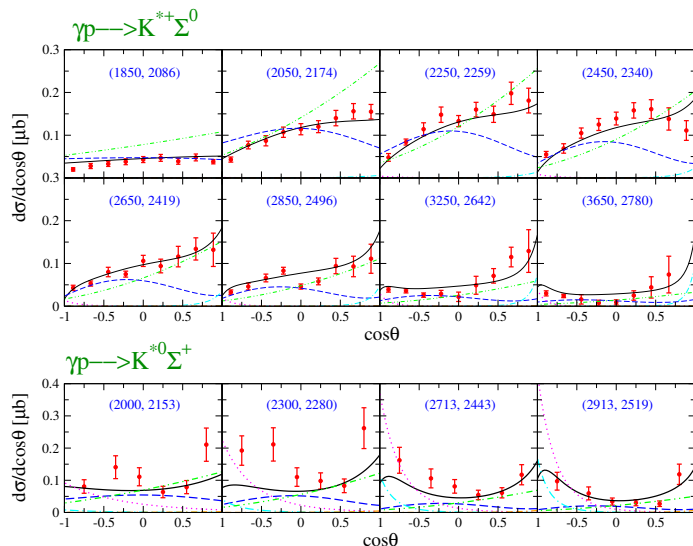


**Figure 2.** Differential cross sections for  $\gamma p \rightarrow K^{*+}\Sigma^0$  and  $\gamma p \rightarrow K^{*0}\Sigma^+$  as a function of  $\cos \theta$  (black solid lines) in model I. The scattered symbols denote the CLAS data [1, 2]. The blue dashed and green dash-double-dotted lines represent the individual contributions from the  $\Delta(1905)5/2^+$  and  $\Delta$  exchanges, respectively. The magenta dotted and cyan dash-dotted lines represent the individual contributions from the  $\Lambda$  and  $K^*$  exchanges for  $\gamma p \rightarrow K^{*+}\Sigma^0$ , and the  $\Sigma$  and  $\Sigma^*$  exchanges for  $\gamma p \rightarrow K^{*0}\Sigma^+$ , respectively. The numbers in parentheses denote the centroid value of the photon laboratory incident energy (left number) and the corresponding total center-of-mass energy of the system (right number), in MeV.

The results for differential and total cross sections obtained in model I are presented in Figs. 2-3. One sees that for  $\gamma p \rightarrow K^{*+}\Sigma^0$ , the  $\Delta(1905)5/2^+$  and  $\Delta$  exchanges provide dominant contributions at low energies, the  $K^*$  exchange contributes significantly at high energy forward angles, and the  $\Lambda$  exchange offers small contributions at high energy backward angles. For  $\gamma p \rightarrow K^{*0}\Sigma^+$ , the  $\Delta$  exchange provides dominant contributions, the  $\Delta(1905)5/2^+$  and  $\Sigma$  exchanges contribute significantly at low energies and high energy backward angles, respectively, and the  $\Sigma^*$  exchange offers considerable contributions at high energy backward angles.

The results for differential and total cross sections obtained in model II are presented in Figs. 4-5. One sees that for  $\gamma p \rightarrow K^{*+}\Sigma^0$ , the  $\Delta(1905)5/2^+$  exchange provides dominant

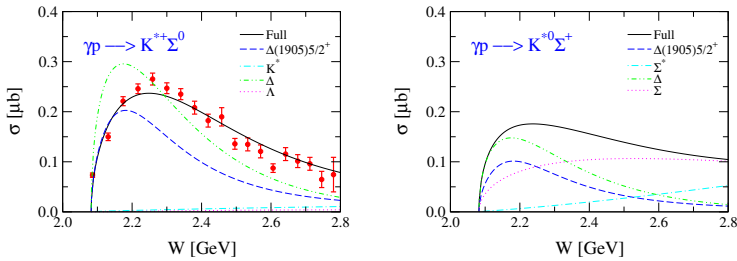


**Figure 3.** Total cross sections with dominant individual contributions for  $\gamma p \rightarrow K^{*+}\Sigma^0$  and  $\gamma p \rightarrow K^{*0}\Sigma^+$  in model I. Data are from the CLAS Collaboration [1] but not included in the fit.

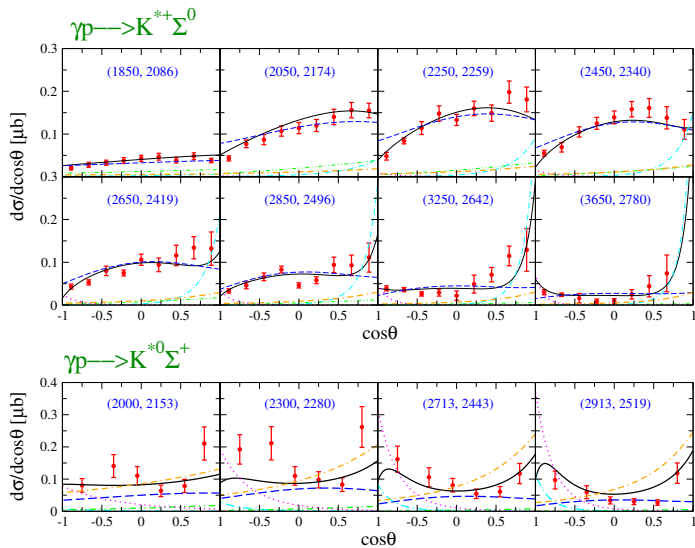


**Figure 4.** Differential cross sections for  $\gamma p \rightarrow K^{*+}\Sigma^0$  and  $\gamma p \rightarrow K^{*0}\Sigma^+$  as a function of  $\cos \theta$  (black solid lines) in model II. Notations are the same as in Fig. 2 except that the orange dot-double-dashed lines represent the  $\kappa$  exchange.

contributions at low energies, the  $K^*$  and  $\kappa$  exchanges contribute significantly and considerably, respectively, at high energy forward angles, and the  $\Lambda$  exchange offers supplementary contributions at high energy backward angles. For  $\gamma p \rightarrow K^{*0}\Sigma^+$ , the  $\kappa$  exchange provides substantial contributions especially at forward angles, the  $\Delta(1905)5/2^+$ ,  $\Sigma$ , and  $\Sigma^*$  exchanges have similar contributions as in model I.

The computed spin density matrix elements for  $\gamma p \rightarrow K^{*0}\Sigma^+$  at  $E_\gamma = 1.85 - 2.96$  GeV obtained in model I and model II are presented in Fig. 6. One sees that although there is only one data point at very forward angle for each observable, our theoretical values agree well with the corresponding data.

In Fig. 7 we show our calculated results for the parity spin asymmetry for  $\gamma p \rightarrow K^{*0}\Sigma^+$  at  $E_\gamma = 1.85 - 2.96$  GeV. The parity spin asymmetry is defined as  $P_\sigma = 2\rho_{1-1}^1 - \rho_{00}^1$ . If there is only  $t$ -channel interaction, then  $P_\sigma$  tends towards 1 for natural parity exchange and -1 for unnatural parity exchange. In Ref. [4] it was argued that the  $\gamma p \rightarrow K^{*0}\Sigma^+$  is dominated by  $\kappa$  exchange as the observed  $P_\sigma$  is very close to 1. In the present work, for  $\gamma p \rightarrow K^{*0}\Sigma^+$ , we

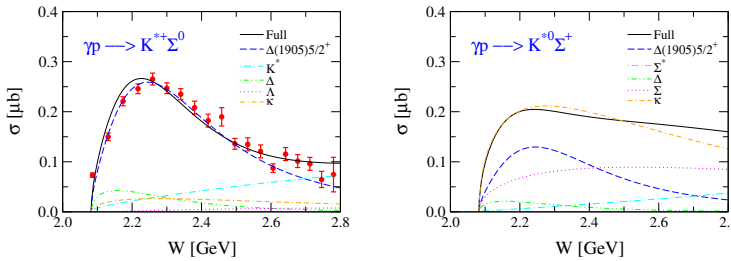


**Figure 5.** Total cross sections with dominant individual contributions for  $\gamma p \rightarrow K^{*+}\Sigma^0$  and  $\gamma p \rightarrow K^{*0}\Sigma^+$  in model II. Data are from the CLAS Collaboration [1] but not included in the fit.

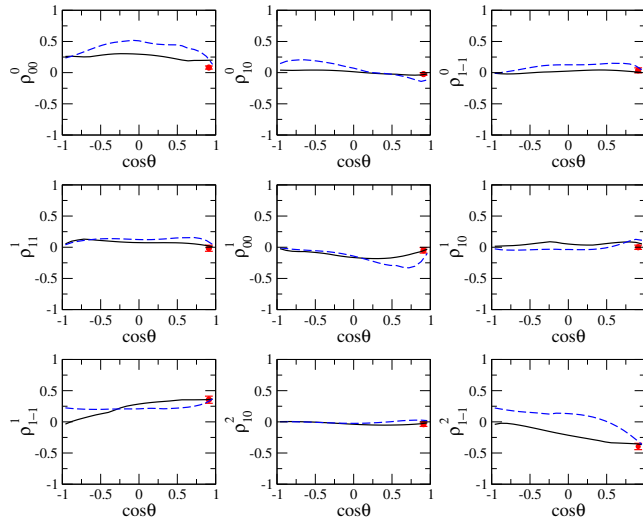


**Figure 6.** Spin density matrix elements for  $\gamma p \rightarrow K^{*0}\Sigma^+$  as a function of  $\cos \theta$  at  $E_\gamma = 1.85 - 2.96$  GeV in model I (solid lines) and model II (dashed lines). Data are from the LEPS Collaboration [4].

have dominant contributions from  $\kappa$  exchange in model II, while in model I the  $\Delta$  exchange dominates the contributions at forward angles but the contributions from  $\kappa$  exchange are rather supplementary. However, as we can see from Fig. 7, in both model I and model II, the theoretical results for  $P_\sigma$  agree well with the data point. This means that the available  $P_\sigma$  data is not sufficient to support the argument that the  $\kappa$  exchange has dominant contributions in the  $\gamma p \rightarrow K^{*0}\Sigma^+$  reaction. Note that in the energy region considered, there are also contributions from  $s$ - and  $u$ -channel interactions. Thus the analysis based on the contributions from pure  $t$ -channel amplitudes to  $P_\sigma$  is not valid.

In Ref. [9], the contributions from the  $N(2080)3/2^-$  and  $N(2270)3/2^-$  states instead of the  $\Delta(1905)5/2^+$  resonance as chosen in Refs. [8, 10] and the present work were considered for  $K^*\Sigma$  photoproduction reactions. The  $N(2080)3/2^-$  and  $N(2270)3/2^-$  are assumed to be the  $K^*\Sigma$  and  $K^*\Sigma^*$  molecules, respectively. The data were well described, indicating that the considered data are compatible with the molecular scenarios of the  $N(2080)3/2^-$  and  $N(2270)3/2^-$  states. It is worthy mentioning that the contributions from the  $\kappa$  exchange in Ref. [9] are also rather small, as observed in model I of the present work, thus not supporting the statement made in Ref. [4] that the  $\gamma p \rightarrow K^{*0}\Sigma^+$  reaction is dominated by the  $\kappa$  exchange.

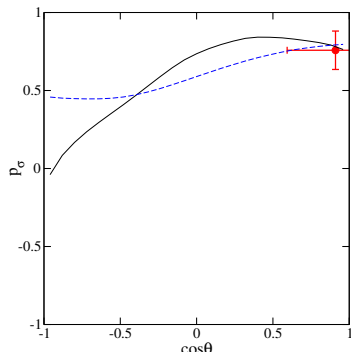


**Figure 7.** Parity spin asymmetry  $P_\sigma$  for  $\gamma p \rightarrow K^{*0}\Sigma^+$  as a function of  $\cos \theta$  at  $E_\gamma = 1.85 - 2.96$  GeV in model I (solid lines) and model II (dashed lines). Data are from the LEPS Collaboration [4].

## 4 Summary and conclusions

In the present work, all the available data on differential cross sections, total cross sections, spin density matrix elements, and parity spin asymmetry for the  $\gamma p \rightarrow K^{*+}\Sigma^0$  and  $\gamma p \rightarrow K^{*0}\Sigma^+$  reactions are well reproduced within an effective Lagrangian approach. The reaction amplitudes are constructed by considering the  $s$ -channel exchanges of  $N$ ,  $\Delta$ , and  $\Delta(1905)5/2^+$ , the  $t$ -channel exchanges of  $K$ ,  $K^*$ , and  $\kappa$ , the  $u$ -channel exchanges of  $\Lambda$ ,  $\Sigma$ , and  $\Sigma^*$ , and the interaction current. Two fits with different reaction mechanisms are obtained that describe the data equally well. The  $s$ -channel  $\Delta(1905)5/2^+$  resonance exchange is found to provide dominant contributions in both fits. The  $t$ -channel  $\kappa$  exchange only contributes significantly to  $\gamma p \rightarrow K^{*0}\Sigma^+$  in model II, which challenges the argument made in Ref. [4] that the available parity spin asymmetry data supports the substantial contribution of  $\kappa$  exchange in  $\gamma p \rightarrow K^{*0}\Sigma^+$ .

## Acknowledgements

This work is partially supported by the National Natural Science Foundation of China under Grants No. 12175240, No. 12305097, and No. 12305137, and the Fundamental Research Funds for the Central Universities.

## References

- [1] W. Tang et al. (CLAS), Phys. Rev. C **87**, 065204 (2013)
- [2] I. Hleiqawi et al. (CLAS), Phys. Rev. C **75**, 042201 (2007), [Erratum: Phys. Rev. C **76**, 039905 (2007)]
- [3] M. Nanova et al. (CBELSA/TAPS), Eur. Phys. J. A **35**, 333 (2008)
- [4] S.H. Hwang et al., Phys. Rev. Lett. **108**, 092001 (2012)
- [5] Q. Zhao, J.S. Al-Khalili, C. Bennhold, Phys. Rev. C **64**, 052201 (2001)
- [6] Y. Oh, H. Kim, Phys. Rev. C **74**, 015208 (2006)
- [7] S.H. Kim, S.i. Nam, A. Hosaka, H.C. Kim, Phys. Rev. D **88**, 054012 (2013)
- [8] A.C. Wang, W.L. Wang, F. Huang, Phys. Rev. C **98**, 045209 (2018)
- [9] D. Ben, A.C. Wang, F. Huang, B.S. Zou, Phys. Rev. C **108**, 065201 (2023)
- [10] A.C. Wang, N.C. Wei, F. Huang, In preparation